COMMISSIONS 27 AND 42 OF THE IAU
INFORMATION BULLETIN ON VARIABLE STARS
Number 6002

Konkoly Observatory
Budapest
20 October 2011

HU ISSN 0374 – 0676

PHOTOMETRIC ANALYSIS OF V400 LYRAE

MARINO, GIUSEPPE [1,2]

[1] Gruppo Astrofili Catanesi - via Milo, 28 I-95125 Catania, ITALY, e-mail: `giumar69@gmail.com`

[2] Sezione Stelle Variabili – Unione Astrofili Italiani (UAI)

During 2010 I observed the EW-type eclipsing binary star V400 Lyrae with the aim of obtaining, for the first time, its physical parameters.

The data were acquired in five nights with a 0.20m Newtonian telescope equipped with a *SBIG ST-7XME* CCD camera provided with BVR_CI_C Johnson–Cousins *Custom Scientific* photometric filters.

At the beginning of each night, before starting the target's observing sequence, I observed standard stars in the open cluster IC 4665. For the target's images, the exposure times were 50–100 s (see the inset in Figure 2).

The CCD images were first corrected for dark and flat field frames; then, the following operations were performed:

- computation of the transformation coefficients to the Johnson–Cousins standard system through IC 4665 standards;
- determination of the magnitudes of four local comparison stars present in each image on the target;
- extraction and color-correction of the differential magnitudes of V400 Lyr;
- standard photometry of V400 Lyr with the help of the magnitudes of the local comparisons.

The dispersion of the magnitude data points was typically better than $0\overset{m}{.}02$–$0\overset{m}{.}03$. Some phase smearing was noted at the minima of the light curve for the 100 s exposures with the higher S/N ratio. However, the issue is generally indistinct in the noise.

I used atmospheric absorption coefficients computed, on each night, by means of the comparison stars observed in a suitable range of airmass. Zero points and color transformation coefficients were computed by analyzing the images of the standard stars in IC 4665 (Menzies & Marang 1996).

Differential and standard photometry were performed by using *MPO Canopus/PhotoRed* software. To evaluate the dependence on the specific procedure adopted, for one night I also performed the photometric reduction using *Iris* software, to extract the stellar fluxes subsequently converted into instrumental and standard magnitudes. These magnitudes are consistent with the results obtained with *MPO Canopus/PhotoRed*, with only a systematic shift within $0\overset{m}{.}01$, also using different photometric apertures.

The intrinsic precision of the procedure was also estimated applying the extraction of the magnitudes on the same standard stars of IC 4665, obtaining a standard deviation of $0\overset{\mathrm{m}}{.}01$ compared to the magnitudes tabulated by Menzies & Marang (1996).

The calibrated standard magnitudes of the comparison stars, obtained on three nights, are reported in Table 1; the RMSs of the comparison stars' magnitudes for corresponding stars are $\sim 0\overset{\mathrm{m}}{.}01$ and $\sim 0\overset{\mathrm{m}}{.}05$, respectively on those three nights and on all the five nights. The mean discrepancies of my magnitudes reported in Table 1 with respect to the values reported on MPOSC3 (the internal catalog of *MPO Canopus/PhotoRed* described in the user manual) are $0\overset{\mathrm{m}}{.}045$, $0\overset{\mathrm{m}}{.}023$, $0\overset{\mathrm{m}}{.}010$ and $0\overset{\mathrm{m}}{.}006$, respectively in the B, V, R_C and I_C bands.

To superimpose the data of different nights in a unique phased light curve, a revision of the ephemeris was necessary because of the period variation clearly evident in the O–C diagram present in the B.R.N.O. O–C *Gateway* web page (`http://var.astro.cz/ocgate`). No dependence of the O–C on the minimum type (primary or secondary) is evident, accounting for a half period difference between the two minima type, assuming phase 0.5 for secondary minima.

The linear best fit of the times of minimum spanning in the range 2009–2010 (Figure 1), leads to the following ephemeris:

$$\mathrm{T_{min}\ (HJD) = 2452500.084759(\pm 0.00164) + 0.25342419(\pm 0.00000015) \times E}$$

The first important step in my physical and geometrical analysis of V400 Lyr was to estimate its intrinsic colors.

As seen in Figure 2, the minimum at phase 0 (primary) is flatter (and slightly deeper) than the secondary one, so the star occulted at phase 0 should be smaller than its companion, and the orbital inclination should be near to 90° (total occultation).

The observed color indices at phase 0, quoted in the first line of Table 2, suggest a spectral classification in the ranges K1 V – K2 V (dwarfs), G9 IV – K1 IV (subgiants) and G5 III – G7 III (giants). We have to discard subgiant and giant stars, because they are incompatible with a period of $0\overset{\mathrm{d}}{.}25$. However, the observed color indices do not fit well a unique spectral type; this, coupled with the faint magnitude of the star (which indicates a distance larger than one hundred parsec), strongly suggests that this star is reddened by interstellar matter.

Thus, I computed all the possible dereddened colors, by letting the color excess $E(B-V)$ parameter free to vary from 0 to 0.60 in steps of 0.01. The color excesses $E(V-R)$ and $E(V-I)$ were deduced from $E(B-V)$ on the base of the relation represented in Figure 7 of Fitzpatrick (1999) assuming R=3.1. Comparing the dereddened colors at phase 0 with the expected ones for the various spectral types, I verified that the best fits is achieved for $E(B-V) \sim 0.11$ and spectral type between G8 V and K0 V.

The value of $E(B-V) = 0.11$ implies a distance of 0.43 kpc if we assume a standard reddening law $A(V) = 3.1 \times E(B-V)$ and an extinction value in V band of 0.8 mag/kpc typical of the Cygnus region (Mikolajewska & Mikolajewski 1980).

Table 1 Standard magnitudes and color indexes for the comparison stars

Star NOMAD1	$\alpha_{2000.0}$ hh:mm:ss	$\delta_{2000.0}$ ° ′ ″	V	$B-V$	$V-R_\mathrm{C}$	$V-I_\mathrm{C}$
1281-0377168	19:13:48.4	+38 07 57	11.777 ± 0.023	1.068 ± 0.019	0.575 ± 0.009	1.106 ± 0.009
1282-0369640	19:13:26.0	+38 16 12	12.158 ± 0.025	0.691 ± 0.021	0.412 ± 0.010	0.808 ± 0.011
1281-0377481	19:14:09.5	+38 07 19	11.584 ± 0.025	0.414 ± 0.014	0.246 ± 0.009	0.474 ± 0.011
1280-0380056	19:14:04.9	+38 00 13	11.632 ± 0.024	0.995 ± 0.019	0.535 ± 0.009	1.012 ± 0.009

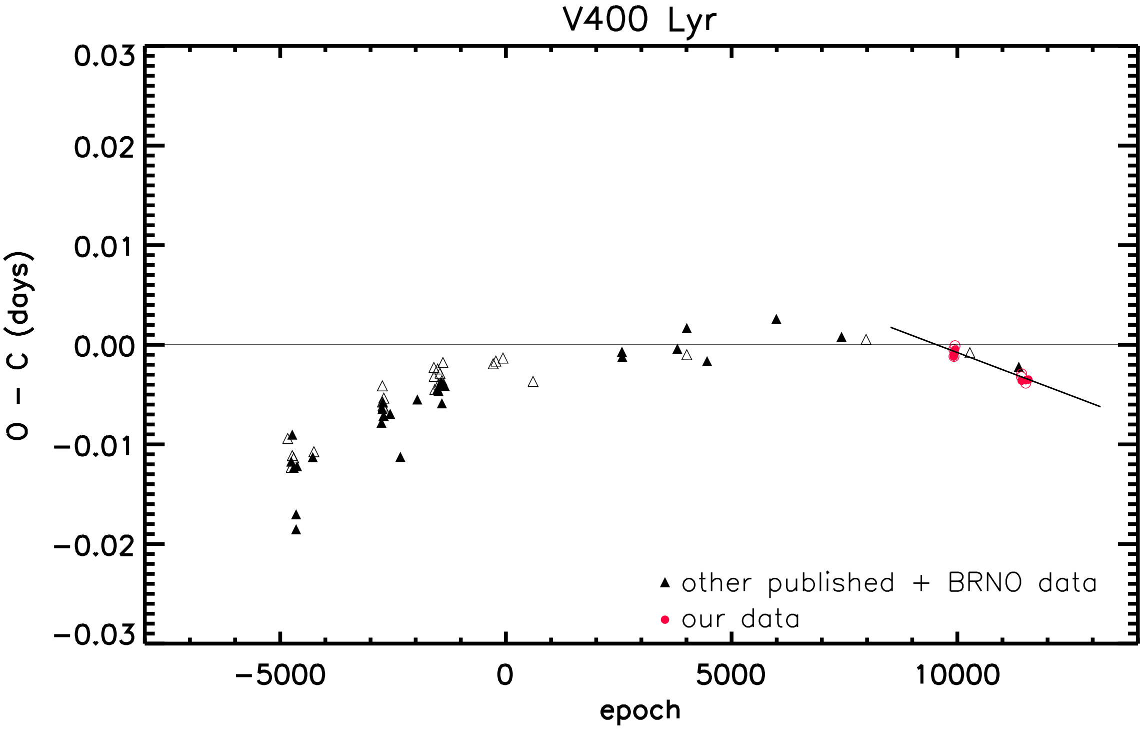

Figure 1. O−C diagram for V400 Lyr, assuming the ephemeris given in the web site of Kreiner (2004). Empty symbols are for secondary minima. The linear best fit for data spanning in the range 2009–2010 is shown. As "our data" are also considered the minima obtained by Marino et al. (2010).

Table 2 Observed and dereddened V magnitude and colors during the primary minimum of V400 Lyr

$E(B-V)$	V	$B-V$	$V-R_C$	$V-I_C$
0.00	13.32	0.859 ± 0.02	0.523 ± 0.01	0.998 ± 0.02
0.08	13.07	0.78	0.44	0.87
0.11	12.99	0.75	0.41	0.82

The comparison between dereddened V magnitude at the primary minimum and absolute magnitudes expected for G8 V – K0 V stars suggests $E(B-V) \sim 0.08$ and spectral type ~K0 V.

Combining the previous considerations, it is reasonable to assume a temperature $T = 5300 \pm 100$ K for the "2" star visible at phase 0.

The following step of the analysis consisted in searching for the geometrical and surface model of the two eclipsing components to best reproduce the shape of each light curve. With this aim, I used PHOEBE software (Prsa & Zwitter 2005). A preliminary solution was found by using the v0.31a version for Windows, that is the latest stable publicly available version; after, the v0.32 subversion for Windows was used to find the final solution.

To give a relative weight to the different BVR_CI_C light curves, for each photometric band I considered not only the photometric error in each individual point, but also the average of residuals with respect to the best fit solution. However, the resulting solution was found very similar to the fit of unweighted curves.

The shape of an eclipsing binary light curve essentially depends on *relative* quantities (star "2" with respect to star "1"); for instance, relative mass, relative size and relative effective temperature can be deduced. However, my estimation of distance and spectral type allows an absolute scaling of the system which is good enough to establish limb and gravity darkening coefficients, respectively x and g, typically tabulated as function of effective temperature and log g. The separation of the components, necessary to absolutely calibrate masses and sizes, was (approximately) obtained iteratively adjusting it up to obtain a bolometric magnitude consistent with the expected value for a G9 V spectral type, assumed for the component occulting visible at phase 0 (*secondary star* in the PHOEBE convention); distance and dereddened V observed magnitude were also taken into account. However, the best and more secure way to get an absolute scale for the system is to obtain the radial velocity curve of both components, which would require a telescope with a much larger aperture.

For each photometric band, linear limb darkening coefficients were assumed interpolating the values tabulated by van Hamme (1993) for solar abundances. Bolometric albedo was assumed to be 0.60. No third light was allowed and circular orbit and synchronous rotation were assumed. Gravity darkening was assumed as the average of the values recently given by Claret & Bloemen (2011) for different bands, which are considerably different from the value of $g = 0.32$, typically adopted in previous light curve modellings. By using $g = 0.32$, the temperature found is about 30 K higher, but similar values for the other fitted parameters and cost function were found. Negligible differences are obtained considering more complex expressions for the limb-darkening, such as quadratic or square-root laws.

The simultaneous fit of the BVR_CI_C light curves was run using Differential correction method, stopping the iterations at the minimum value of the cost function. To avoid remaining trapped in local minima in the parameter space, several different starting pa-

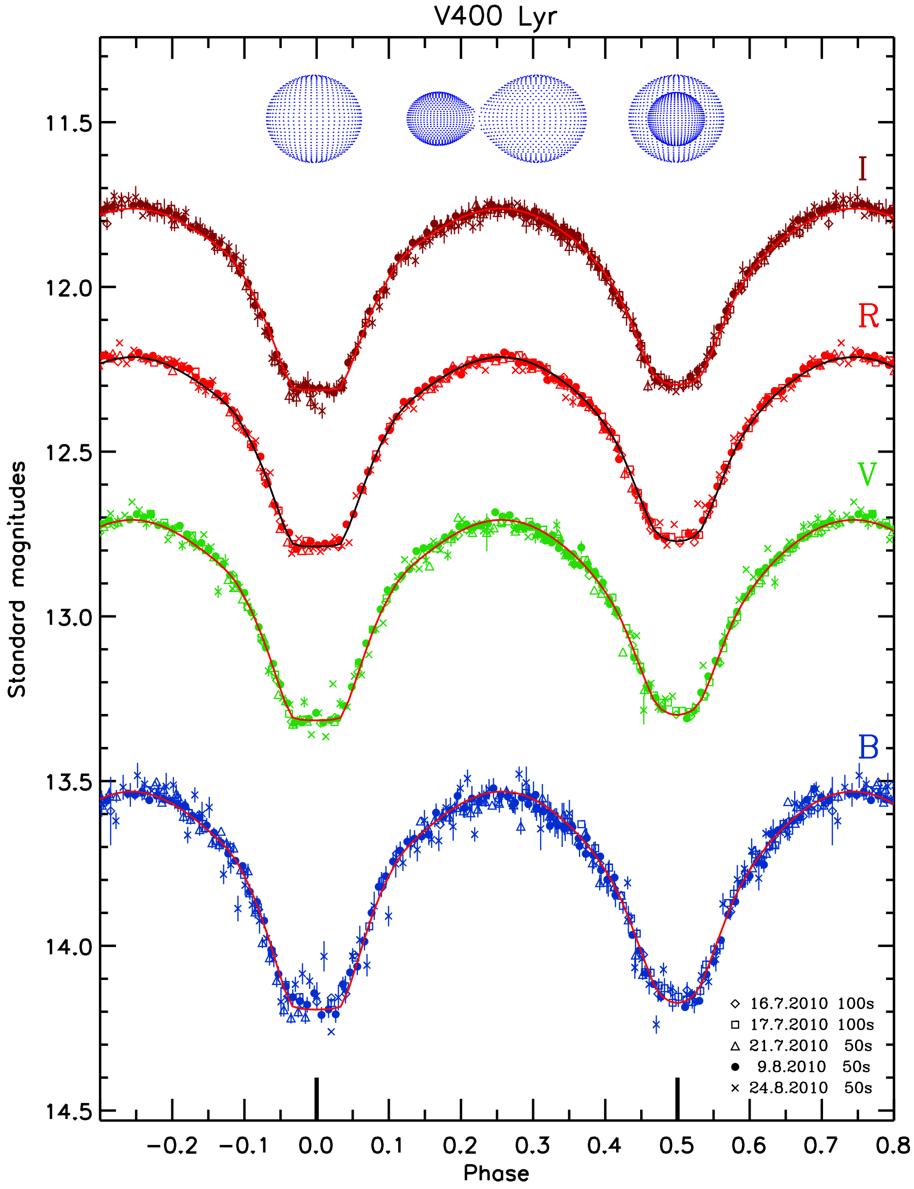

Figure 2. $BVR_{\mathrm{C}}I_{\mathrm{C}}$ photometry of V400 Lyr. The synthetic light curves are shown as continuum line. The stellar configuration is represented at the phases 0.00, 0.25 ad 0.50. The (original not scaled) error bars are shown for errors larger than $0\overset{\mathrm{m}}{.}015$.

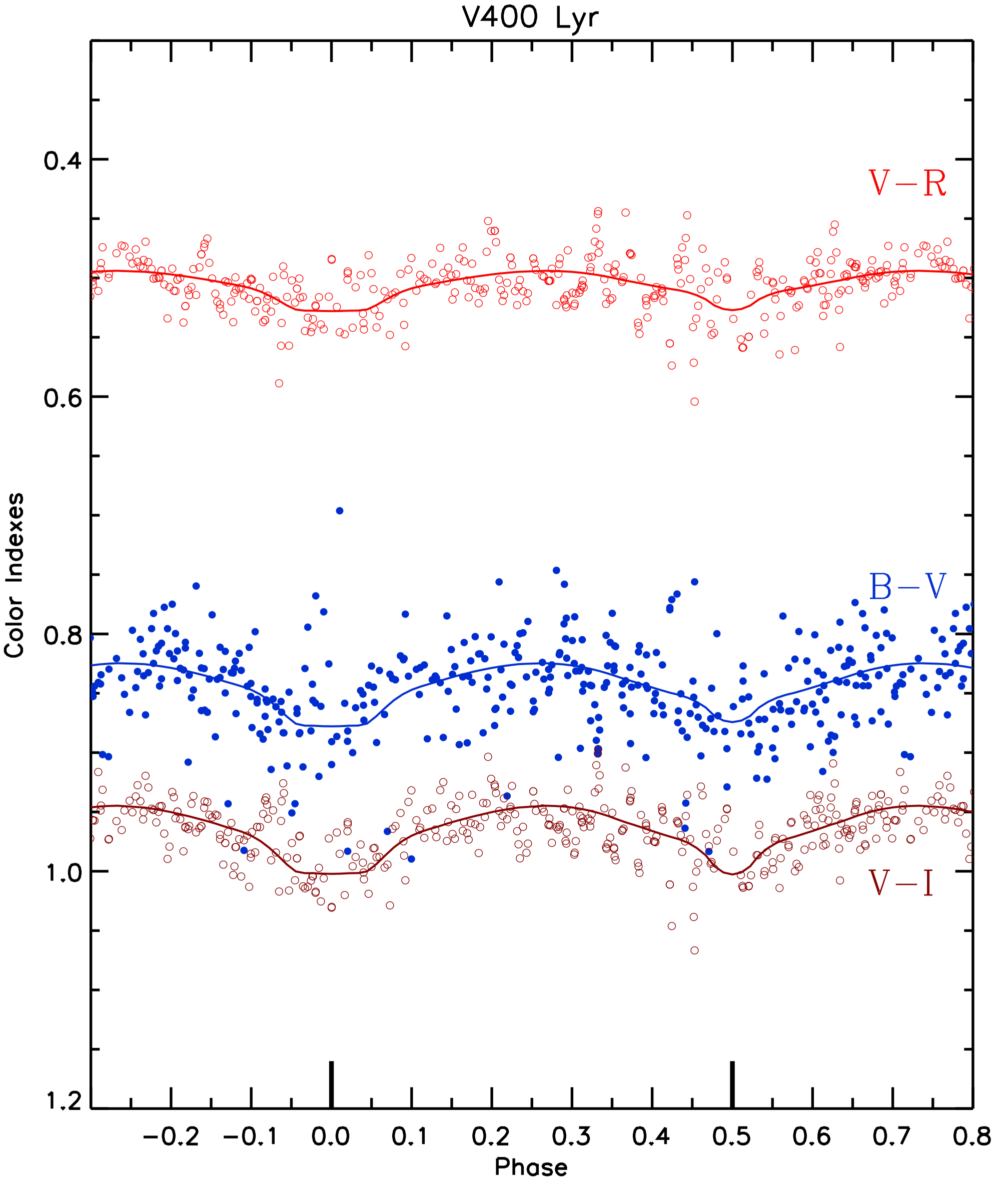

Figure 3. Color indices of V400 Lyr.

rameters were tried. Also running the Simplex method, the same region of the parameters' space was reached.

By adopting the "Overcontact binary of the W UMa type" Mode (that assumes thermal equilibrium between the two components) the solution found for mass ratio $q < 1$ is able to reproduce the different depths of the minima, but it shows a flatter minimum at phase 0.5, unlike the observed light curve. Instead, the solution obtained assuming $q > 1$ reproduces the flat minimum at phase 0, but it presents the deeper minimum at phase 0.5. Only by setting the "Overcontact binary not in thermal contact" Mode, is possible to correctly fit depth and shape of the minima (for $q > 1$).

As usual, the light curve modelling *does not* fit the relative shift between different photometric bands (i.e. the color indices), being the level of each synthetic curve optimized on the corresponding observed light curve, which is internally normalized by the fitting program. Thus, the light curve solutions are shifted to be superimposed on the observed light curves.

Figure 2 shows the best fit to the $BVR_\mathrm{C}I_\mathrm{C}$ light curves versus phase.

The geometrical representation of the system is given in the same Figure 2 for three different phases.

The color indices are shown in Figure 3; the continuum lines represent the synthetic curves obtained as the difference of the synthetic magnitudes.

The resulting fit indicates V400 Lyr is a W-type W UMa contact binary, being the larger secondary in front of the smaller primary component at the primary minimum.

It is useful to recall that radial velocity measures are strongly necessary to obtain an accurate absolute determination of masses and sizes. However, in the final rows of Table 3, possible absolute values are reported, deduced from the light curve model assuming that the secondary component is similar to a G9 V star. We note that the mass and the radius for the primary (hotter and smaller) star is much smaller than expected values typical of a main sequence star with effective temperature of $\sim$ 5450 K. This is probably a consequence of stellar evolution strongly influenced by mass exchange and, eventually, by mass loss. In fact, stellar masses agree with the empirical relation given by Gazeas & Niarchos (2006) for contact binaries.

The asymmetry visible in B and V bands near the bottom of the secondary minimum is probably due to cool spots on the cooler star.

References:

Claret, A., Bloemen, S., 2011, *A&A*, **529**, A75
Fitzpatrick, E. L., 1999, *PASP*, **111**, 63
Gazeas, K. D., Niarchos, P. G., 2006, *MNRAS*, **370**, L29
Kreiner, J. M., 2004, *AcA*, **54**, 207, `http://www.as.up.krakow.pl/ephem`
Marino, G., *et al.*, 2010, *IBVS*, **5917**, 1
Menzies, J. W., Marang, F., 1996, *MNRAS*, **282**, 313
Mikolajewka, J., Mikolajewki, M., 1980, *AcA*, **30**, 347
Prsa, A., Zwitter, T., 2005, *ApJ*, **628**, 426
van Hamme, W., 1993, *AJ*, **106**, 2096

Table 3 Physics and geometrical elements of V400 Lyr

Parameter	Value	Error[1]
i	$89\overset{\circ}{.}6$	$0\overset{\circ}{.}2$ (1°)
T_1	5450 K	(110 K)[2]
T_2	5300 K	(assumed)
$q = M_2/M_1$	2.97	0.01 (0.1)
$\Omega_1 = \Omega_2$	6.47	0.01 (0.1)
g_1	0.48	(assumed)
g_2	0.51	(assumed)
$x_1(B)$	0.79	(assumed)
$x_1(V)$	0.65	(assumed)
$x_1(R_\mathrm{C})$	0.54	(assumed)
$x_1(I_\mathrm{C})$	0.44	(assumed)
$x_1(bol)$	0.52	(assumed)
$x_2(B)$	0.81	(assumed)
$x_2(V)$	0.68	(assumed)
$x_2(R_\mathrm{C})$	0.56	(assumed)
$x_2(I_\mathrm{C})$	0.46	(assumed)
$x_2(bol)$	0.53	(assumed)
A_1	0.6	(assumed)
A_2	0.6	(assumed)
$L_2/L_1(B)$	2.195	0.009 (0.04)
$L_2/L_1(V)$	2.295	0.007 (0.04)
$L_2/L_1(R_\mathrm{C})$	2.365	0.008 (0.04)
$L_2/L_1(I_\mathrm{C})$	2.414	0.008 (0.04)
(from q and Ω)		
R_1/a	0.301	(0.06)
R_2/a	0.488	(0.06)
(assuming $a = 1.80R_\odot$)[3]		
M_1	$0.31M_\odot$	$(0.01M_\odot)$
M_2	$0.91M_\odot$	$(0.01M_\odot)$
R_1	$0.54R_\odot$	$(0.1R_\odot)$
R_2	$0.88R_\odot$	$(0.1R_\odot)$
M_{bol-1}	6.3	(0.4)
M_{bol-2}	5.4	(0.3)

[1] Formal errors from the differential corrections solution. In bracket, heuristic approximated errors based on the cost function's trend.

[2] Essentially derived from the uncertainty on T_2.

[3] Absolute values should be regarded as preliminary estimates, due to unavailability of radial velocities.